

1 **Title: Antibacterial activity of tamoxifen derivatives against methicillin-resistant**

2 *Staphylococcus aureus*

3

4 **Authors:** Irene Molina Panadero,¹ Javier Falcón Torres,¹ Karim Hmadcha,^{2,3} Salvatore
5 Princiotta,⁴ Luigi Cutarella,⁵ Mattia Mori,⁵ Sabrina Dallavalle,⁴ Michael S.
6 Christodoulou,^{4*} and Younes Smani^{1,2*}

7

8 **Affiliations:**

9 ¹Centro Andaluz de Biología del Desarrollo, Universidad Pablo de Olavide/Consejo
10 Superior de Investigaciones Científicas/Junta de Andalucía, Sevilla, Spain,

11 ²Departamento de Biología Molecular e Ingeniería Bioquímica, Universidad Pablo de
12 Olavide, Sevilla, Spain,

13 ³Biosanitary Research Institute (IIB-VIU), Valencian International University (VIU),
14 Valencia, Spain,

15 ⁴Department of Food, Environmental and Nutritional Sciences (DeFENS), University of
16 Milan, via Celoria 2, 20133 Milan, Italy.

17 ⁵Department of Biotechnology, Chemistry and Pharmacy, University of Siena, via Aldo
18 Moro 2, 53100 Siena, Italy.

19

20 ***Corresponding author:**

21 **Michael S. Christodoulou:** Department of Food, Environmental and Nutritional
22 Sciences (DeFENS), University of Milan, via Celoria 2, 20133 Milan, Italy. Email:
23 michail.christodoulou@unimi.it

24 **Younes Smani:** Andalusian Center of Developmental Biology, CSIC, University of
25 Pablo de Olavide, Department of Molecular Biology and Biochemical Engineering,

26 University of Pablo de Olavide, Seville, Carretera de Utrera Km 1, 41013, Seville,

27 Spain. Tel: +34-954349051, E-mail: ysma@upo.es.

28

29 **Running title:** Tamoxifen derivatives against *S. aureus*

30

31 **ABSTRACT**

32 The present work aimed to discover new tamoxifen derivatives with antimicrobial
33 potential, particularly targeting methicillin-resistant *Staphylococcus aureus* (MRSA).

34 The MIC of 22 tamoxifen derivatives was determined against *S. aureus* reference and
35 MRSA strains, using microdilution assays. The antibacterial effects of selected
36 tamoxifen derivatives against MRSA (USA7) were assessed through bacterial growth
37 assays. Bacterial membrane permeability and molecular docking assays were
38 performed.

39 The MIC of the tamoxifen derivatives against MRSA ranged from 16 to >64 µg/mL.
40 Bacterial growth assays demonstrated that tamoxifen derivatives **2**, **5**, and **6** reduced
41 dose-dependently the growth of the USA7 strain. Moreover, treatment of MRSA with
42 derivatives **2** and **5** resulted in increased membrane permeabilization without being the
43 cell wall their molecular target.

44 These data suggest that tamoxifen derivatives exhibit antibacterial activity against
45 MRSA, potentially broadening the spectrum of available drug treatments for combating
46 antimicrobial-resistant Gram-positive bacteria.

47

48 **Keywords:** *Staphylococcus aureus*, tamoxifen derivatives, resistance, infection,
49 treatment.

50

51 **Importance**

52 The development of new antimicrobial therapeutic strategies requires immediate
53 attention to avoid the tens of millions of deaths predicted to occur by 2050 as a result of
54 multidrug-resistant (MDR) bacterial infections. In this study, we assessed the
55 antibacterial activity of 22 tamoxifen derivatives against methicillin-resistant
56 *Staphylococcus aureus* (MRSA). We found that three tamoxifen derivatives exhibited
57 antibacterial activity against MRSA clinical isolats, presenting MIC₅₀ values between
58 16 and 64 µg/mL and reducing bacterial growth over 24 h. Additionally, this
59 antibacterial activity for two of the derivatives was accompanied by increased
60 membrane permeability of MRSA. Our results suggest that tamoxifen derivatives might
61 be used as a potential therapeutic alternative for treating MRSA strains in an animal
62 model of infection.

63

64 INTRODUCTION

65 In the last decades, Gram-positive bacteria have demonstrated an increasing
66 antimicrobial resistance, driven by various genomic, transcriptomic, and proteomic
67 adaptations¹. This alarming trend aligns with a concerning decline in the development
68 of new antibiotics, a phenomenon often referred to as the “Post-Antibiotic Era”². This
69 situation underscores the urgent need for effective solutions, a concern highlighted by
70 numerous institutions (ref). Consequently, there is a growing demand for innovative
71 antimicrobial therapeutic approaches, including the exploration of non-antibiotic
72 compounds and drug repurposing, both as monotherapy and in combination with the
73 limited clinically relevant antibiotics currently available³.

74 Among the various strategies employed in the discovery of new antibacterial agents,
75 drug repurposing is one of the most exploited³. A very representative example of such
76 approach is tamoxifen, a well-known chemotherapeutic drug, widely used for decades as
77 the gold standard for the treatment of estrogen receptor positive breast cancers and
78 related metastatic forms⁴. Recently, tamoxifen has exhibited relevant antibacterial
79 properties against a range of pathogenic microorganisms, including Gram-positive
80 *Staphylococcus epidermidis*, and *Enterococcus faecalis* and Gram-negative *Escherichia*
81 *coli* and *Acinetobacter baumannii*^{5,6}. This antimicrobial effect may be ascribed to the
82 cytochrome P450-mediated metabolism of tamoxifen, resulting in the generation of
83 three major metabolites: *N*-desmethyltamoxifen, 4-hydroxytamoxifen and endoxifen^{5,7}.

84 Only a limited number of studies have reported the activity of these metabolites against
85 various infectious agents^{5,6,8-12}. Among these, 4-hydroxytamoxifen has garnered
86 attention for its chemical behavior as a weak base, since it has been observed that such
87 property is responsible for the protection of cells and mice against lethal Shiga toxin 1
88 (STx1) or Shiga toxin 2 (STx2) toxicosis⁸. It has also demonstrated efficacy against
89 *Plasmodium falciparum* and *Cryptococcus neoformans*^{10,11}. Furthermore, when used in

90 monotherapy, 4-hydroxytamoxifen has displayed activity against *Mycobacterium*
91 *tuberculosis* (with a MIC₅₀ of approximately 2.5 to 5 µg/mL)¹². Endoxifen's activity was
92 studied against *C. neoformans*, revealing a MIC of 4 µg/mL¹¹. The combination of *N*-
93 desmethyltamoxifen, 4-hydroxytamoxifen and endoxifen exhibited MIC₅₀ values of 8
94 and 16 µg/mL against clinical isolates of *A. baumannii* and *E. coli*, and MIC₅₀ values of
95 1 and 2 µg/mL against clinical isolates of *S. epidermidis* and *E. faecalis*^{5,6}.

96 To identify new chemical compounds with antimicrobial potential, a collection of 22
97 tamoxifen derivatives, bearing different electron-withdrawing or electron-donating
98 substituents on the aromatic rings A and B (Table 1) was tested against methicillin-
99 resistant *S. aureus* (MRSA).

100

101 **RESULTS**

102 **Antimicrobial activity of tamoxifen derivatives**

103 Twenty-two tamoxifen derivatives (Table 1) were subjected to evaluation to determine
104 their MIC against *S. aureus* ATCC 1556 reference strain. Only the tamoxifen
105 derivatives **2**, **5** and **6** showed MIC for *S. aureus* ATCC 1556 strain ranging from 16 to
106 32 µg/mL, while the rest of the compounds did not show MIC values <64 µg/mL (Table
107 1).

108 A comparison between the biological results and the chemical structures of the
109 tamoxifen derivatives allowed some interesting structure-activity relationships
110 outcomes. In particular, the most active compounds **2**, **5** and **6** share the presence of the
111 hydroxyl group in *para* position on both phenyl rings, A and B. All the derivatives
112 bearing the hydroxyl group on only one of the phenyl rings resulted inactive
113 (compounds **13**, **14**, **17**, **18**, **19** and **20**). In the case of no substituents on the phenyl
114 rings (compounds **1**, **9** and **10**) or in presence of electron-donating substituents diverse

115 from the hydroxyl group on one or both phenyl rings A and B, the derivatives resulted
116 inactive as well (compounds **3**, **4**, **7**, **8**, **11**, **12**, **15**, **16**, **21** and **22**).

117 The most promising derivatives were selected on the base of a MIC ≤ 64 $\mu\text{g/mL}$ and
118 were evaluated against 7 clinical isolates of MRSA to extend their biological evaluation
119 to the antimicrobial effect on resistant strains. As shown in Table 2, the MICs of
120 tamoxifen derivatives **2**, **5** and **6** for MRSA strains ranged from 16 to 64 $\mu\text{g/mL}$.

121

122 **Bacterial growth curves**

123 Using bacterial growth, we examined the antibacterial activity of the selected tamoxifen
124 derivatives against MRSA USA7 strain (Figure 1). Compounds **2**, **5** and **6** at
125 concentrations of 1x, 2x and 4x MIC, reduced the growth of this strain in a
126 concentration-dependent manner during 24 h. This antibacterial effect is more
127 pronounced at 2x and 4xMIC.

128

129 **Effect of tamoxifen derivatives on the bacterial cell membrane**

130 In order to determine the mode of action of the selected tamoxifen derivatives, their
131 effect on the membrane permeability of USA7 strain was evaluated by incubation with
132 ethidium homodimer 1, a fluorescent marker known to enter bacterial cells when the
133 membrane integrity is compromised.

134 Fluorescence monitoring using a Typhoon FLA scanner for 3 h showed a slight increase
135 in the cellular fluorescence of the USA7 strain when treated with sub-MIC of the
136 tamoxifen derivatives **2** and **5**, but not for **6**. (Figure 2).

137

138 **Tamoxifen derivatives interaction with bacterial membrane**

139 To investigate the interaction between tamoxifen derivatives **5** and **6** and the bacterial
140 membrane model, and to assess how subtle structural modifications (i.e., *cis/trans*

141 conformation) might affect their ability to embed within the target, unbiased molecular
142 dynamics (MD) simulations were carried out starting from the small molecules being
143 placed in the solvent area.¹³⁻¹⁹

144 Different from previous findings with different scaffolds¹⁷, for derivatives **5** and **6** the
145 density plots clearly evidence that the molecules are unable to penetrate deeply into the
146 membrane model (Figure 3A,B). In fact, density peaks of the two derivatives slightly
147 exceeds the density peak of the phosphates that represent the membrane outermost
148 layer. These results suggest that the *S. aureus* membrane might not be the molecular
149 target of **5** and **6** antibacterial efficacy.

150 To further provide atomistic details of this outcome, the distance between each
151 molecule and the lipid bilayer was monitored along MD trajectories. Then, the MD
152 frame corresponding to the smallest intermolecular distance was extracted and visually
153 inspected. A labile H-bond interaction between the phenol moiety of the molecules and
154 the protonated ammino group (i.e., R-NH₃⁺) of a phosphatidylglycerol residues at the
155 membrane interface with the solvent was observed (Figure 4A,B). Unlike **5**, derivative **6**
156 also establishes an additional interaction with the -OH group of a phosphatidylglycerol
157 residue (Figure 4B). However, this interaction is not stable in time and failed to promote
158 molecules embedding into the *S. aureus* membrane model within the simulation time,
159 which further reinforce the hypothesis that **5** and **6** exploit their antibacterial potentials
160 through the interaction with target that differ from the bacterial membrane.

161

162 **DISCUSSION**

163 The rise of multidrug resistant *S. aureus* has led to a wide use of the last options for the
164 treatment of severe infections caused by this microorganism, and to the consequent
165 acquired antimicrobial resistance worldwide in the last decades²⁰. In previous studies,

166 tamoxifen and its metabolites garnered attention as a potential repurposed drug for
167 treatment of infectious diseases⁹.

168 Due to the antibacterial effect of tamoxifen and its metabolites *N*-desmethyltamoxifen,
169 4-hydroxytamoxifen and endoxifen against *S. epidermidis* and *A. baumannii*^{5,6}, we
170 hypothesized that tamoxifen derivatives may enhance this antibacterial activity against
171 MRSA. For this purpose, twenty-two tamoxifen derivatives were tested against *S.*
172 *aureus* reference strain.

173 Three tamoxifen derivatives **2**, **5** and **6** in monotherapy showed antibacterial activity
174 against MRSA strains being the MIC between 16 and 64 µg/mL, which overall fell
175 within the range of other known antibiotics such as amikacin, teicoplanin, sulfonamides
176 nitrofurantoin^{21,22}. However, none of the rest of tested tamoxifen derivatives exhibited
177 activity against MRSA. Reasons for this difference could be related to the chemical
178 structure of these derivatives, being **2**, **5** and **6** the only compounds bearing the electron-
179 donating hydroxyl group in *para* position on both phenyl rings A and B.

180 The antibacterial activity of tamoxifen derivatives **2** and **5** at 1x, 2x and 4x MIC against
181 MRSA USA7 strain was more pronounced and began earlier than with tamoxifen
182 derivative **6**. This result may be related to the *trans* stereochemistry (structure **A**) of
183 compounds **2** and **5** and their ability to act on the cell wall of *S. aureus*, as observed
184 with tamoxifen metabolites against Gram-negative bacteria⁵. Permeability assays
185 confirm this observation, since tamoxifen derivatives **2** and **5**, but not **6**, produced a
186 slight increase in membrane permeability of MRSA, suggesting that the bacterial cell
187 wall integrity could be affected and could acts as the target of both derivatives. In
188 support of this hypothesis, tamoxifen has been shown to increase the membrane
189 permeability of *Streptococcus pneumoniae* by perturbing the phospholipid bilayer²³.

190 Even though tamoxifen derivatives might affect cell wall permeability, MD simulations
191 have reported that the *S. aureus* membrane might not be the molecular target of these

192 derivatives due to their instability over time. Alternative mechanisms of action, rather
193 than the perturbation of the cell membrane, cannot be ruled out. Of note, in other
194 microorganisms such as fungi, the mechanism of action of the tamoxifen is well-
195 documented and involves its binding to calmodulin^{24,25}. Moreover, the tamoxifen
196 metabolite, 4-hydroxytamoxifen, can potentially inhibit bacterial phospholipase D in *P.*
197 *aeruginosa*²⁶. Additional research focusing on understanding the mechanism of action
198 of the tested tamoxifen derivatives against MRSA would be of significant interest since
199 different chemical structures resulted active on the aforementioned strain, thus
200 providing a better therapeutic efficacy.

201 The antimicrobial activity of the selected derivatives identified in this work hints at a
202 promising potential that deserves to be further explored *in vivo* after determining their
203 pharmacokinetic parameters. However, *in vitro* bacterial growth showed a progressive
204 regrowth of the MRSA USA 7 strain after treatment with these tamoxifen derivatives,
205 suggesting that acquired resistance could take place. Nevertheless, it should be noted
206 that the MICs of tamoxifen derivatives **2**, **5**, and **6** against the USA 7 strain in this
207 bacterial growth condition are 32, 32, and 16 µg/mL, respectively, which are below the
208 original 2x and 4x MIC of the tamoxifen derivatives concentration. Further
209 investigations, including the determination of tamoxifen derivatives concentration
210 during the bacterial growth assay, are necessary to better understand the regrowth of this
211 strain in their presence.

212 In conclusion, this study's findings offer fresh perspectives on the application of a
213 diverse group of tamoxifen derivatives against MRSA, pathogen for which treatment
214 options are dramatically restricted. Despite the promising potential displayed by this
215 novel class of antibacterial compounds, additional research is required to uncover the
216 mechanism of action of these chemical entities. Moreover, determining the ideal dosage

217 that ensures therapeutic effectiveness in managing severe infections caused by
218 multidrug-resistant Gram-positive remains a critical objective.

219

220 **MATERIAL AND METHODS**

221 **Bacterial Strains**

222 A total of 7 MRSA clinical isolates and one *S. aureus* reference ATCC 1556 strain were
223 used in this study²⁷.

224

225 **Antimicrobial agent and tamoxifen derivatives**

226 The small library of tamoxifen derivatives was prepared as described in literature,
227 starting from appropriately substituted benzophenones which underwent McMurry
228 olefination^{28,29}. The structures of the tested compounds are presented in Table 1.

229

230 ***In vitro* susceptibility testing**

231 The MICs of tamoxifen derivatives were determined against reference and MRSA
232 strains in two independent experiments using the broth microdilution method, in
233 accordance with the standard guidelines of the European Committee on Antimicrobial
234 Susceptibility Testing (EUCAST)³⁰. A 5×10^5 cfu/mL inoculum of each strain was
235 cultured in Luria Bertani (LB) and added to U bottom microtiter plates (Deltlab, Spain)
236 containing the studied tamoxifen derivatives. The plates were incubated for 18 h at 37
237 °C. *Pseudomonas aeruginosa* ATCC 27853 was used as the positive control strain.

238

239 **Bacterial growth curves**

240 To determine the antibacterial and synergistic effects, duplicate bacterial growth curves
241 were performed for MRSA USA7 strain. A 1/200 dilution of an overnight bacterial
242 cultures grown in LB at 37 °C with continuous agitation at 180 rpm was performed in

243 LB in 96-well plate in the presence of 1x, 2x and 4x MIC of compounds **2**, **5** and **6**. A
244 drug-free broth was evaluated in parallel as control. Absorbance measurements at 600
245 nm every 20 min for 24 h were conducted using a Tecan spectrophotometer (model
246 XYZ-2000, Austria).

247

248 **Membrane permeability assays**

249 The bacterial cells were grown in LB broth and incubated in the absence or presence of
250 (i) 1x MIC of compounds **2**, **5** and **6** for 3 h. The pellet was harvested by
251 ultracentrifugation at 4600g for 15 min. The bacterial cells were washed with PBS 1X,
252 and after centrifugation in the same condition described before, the pellet was
253 resuspended in 100 μ L of PBS 1X containing 10 μ L of Ethidium Homodimer-1
254 (ThermoFisher, USA). After 10 min of incubation, 100 μ L was placed into a 96-well
255 plate to measure fluorescence for 300 min using a Typhoon FLA 9000 laser scanner
256 (GE Healthcare Life Sciences, USA) and quantified using ImageQuant TL software (GE
257 Healthcare Life Sciences, USA)³¹.

258

259 **Molecular docking assays**

260 The symmetric lipid bilayer membrane of *S. aureus* was built using the CHARMM-GUI
261 Membrane Builder Tool^{13,14}. This system was designed to mimic the phospholipid
262 composition of the *S. aureus* membrane, which consists of 56.8% phosphatidylglycerol
263 (PG), 37.9% Lys-PG, and 5.3% diphosphatidylglycerol (DPG), also referred as
264 Cardiolipin (CL), in agreement with previous molecular dynamics (MD) studies¹⁵⁻¹⁷.
265 Each lipid bilayer contained a total of 95 lipid molecules, positioned with their centers
266 at $z = 0.$, surrounded by a water layer with a thickness of 50 Å. The system was
267 neutralized using Na^+ and Cl^- ions at a concentration of 0.145 M, as suggested by
268 CHARMM-GUI.

269 Derivatives **5** and **6** were drawn using the Sketchpad powered by Marvin JS included in
270 the ligand reader & modeler module of CHARMM-GUI, and were parameterized using
271 the standard CHARMM force field (FF)³². The Multicomponent Assembler tool was
272 used to randomly distribute the small molecules under investigation within the solvent
273 area. The membrane systems containing these small molecules were then parameterized
274 with a membrane thickness of 50 Å and a box XY length of 79.50 Å^{33,34}. Following
275 system construction with CHARMM-GUI, the topology and coordinate files were
276 generated for AMBER^{35,36}.

277 To investigate the interaction between **5** and **6** with the *S. aureus* membrane model, MD
278 simulations were conducted using AMBER22^{37,38}. The initial system was energy
279 minimized for a total of 40000 steps., with the first 1500 steps employing the steepest
280 descent algorithm, followed by the conjugate gradient algorithm for the remaining steps.
281 A non-bonded cut-off of 10Å was used. After energy minimization, each system was
282 gradually heated to 300 K over 900 ps at constant volume using the Langevin
283 thermostat with a collision frequency of 2 ps⁻¹, and then left at 300 K at constant volume
284 for 200 ps. Box density was equilibrated at constant pressure and constant temperature
285 (300 K) over 1 ns using the Berendsen barostat.

286 Following density equilibration, a preliminary 50 ns MD simulation was conducted at
287 constant pressure. Subsequently, MD trajectories were generated for 500 ns. In all MD
288 simulations, no positional restraints were applied.

289 Analysis of MD trajectories was performed using the CPPTRAJ³⁹ program from the
290 AmberTools package. This analysis included calculation of the mass densities of
291 derivatives within the system along the z-axis. Small molecules interactions with the
292 membrane were visually inspected with PyMol⁴⁰.

293

294 **Statistical Analysis**

295 Group data are presented as means \pm standard errors of the means (SEM). The student *t*-
296 test was used to determine differences between means using the GraphPad Prism 9. A *p*-
297 value <0.05 was considered significant.

298

299 **DATA AVAILABILITY**

300 The data that support the findings of this study are available from the corresponding
301 author upon reasonable request.

302

303 **REFERENCES**

- 304 1. Yelin, I. & Kishony, R. Antibiotic resistance. *Cell* **172**, 1136-1136 (2018).
- 305 2. Bagley, N. & Outterson, K. We will miss antibiotics when they're gone. *The New*
306 *York Times*, January 18 (2017).
- 307 3. Canturri, A. M. & Smani, Y. Anthelmintic drugs for repurposing against Gram-
308 negative bacilli infections. *Curr. Med. Chem.* **30**, 59-71 (2022).
- 309 4. Green, K. A. & Carroll, J. S. Oestrogen-receptor-mediated transcription and the
310 influence of co-factors and chromatin state. *Nat. Rev. Cancer* **7**, 713-22 (2007).
- 311 5. Miró-Canturri, A. et al. Repurposing of the tamoxifen metabolites to combat
312 infections by multidrug-resistant gram-negative bacilli. *Antibiotics* **10**, 336 (2021a).
- 313 6. Miró-Canturri, A. et al. Repurposing of the tamoxifen metabolites to treat
314 methicillin-resistant *Staphylococcus epidermidis* and vancomycin-resistant
315 *Enterococcus faecalis* infections. *Microbiol. Spectr.* **9**, e0040321 (2021b).
- 316 7. Klein, D. J. et al. PharmGKB summary: tamoxifen pathway, pharmacokinetics.
317 *Pharmacogenet. Genomics* **23**, 643-647 (2013).
- 318 8. Selyunin, A. S., Hutchens, S., McHardy, S. F. & Mukhopadhyay, S. Tamoxifen
319 blocks retrograde trafficking of Shiga toxin 1 and 2 and protects against lethal
320 toxicosis. *Life Sci. Alliance* **2**, e201900439 (2019).

- 321 9. Montoya, M. C. & Krysan, D. J. Repurposing estrogen receptor antagonists for the
322 treatment of infectious disease. *mBio* **9**, e02272-18 (2018).
- 323 10. Weinstock, A. et al. Tamoxifen activity against *Plasmodium* in vitro and in mice.
324 *Malar. J.* **18**, 378 (2019).
- 325 11. Butts, A. et al. Estrogen receptor antagonists are anti-cryptococcal agents that
326 directly bind EF hand proteins and synergize with fluconazole *in vivo*. *mBio* **5**,
327 e00765-13 (2014).
- 328 12. Chen, F. C. et al. Pros and cons of the tuberculosis drugome approach-an empirical
329 analysis. *PLoS One* **9**, e100829 (2014).
- 330 13. Li Y, Liu J, Gumbart JC. Preparing Membrane Proteins for Simulation Using
331 CHARMM-GUI. In: *Methods in Molecular Biology*. Vol 2302; 2021.
- 332 14. Jo S, Kim T, Iyer VG, Im W. CHARMM-GUI: A web-based graphical user
333 interface for CHARMM. *J Comput Chem.* **29**(11) (2008).
- 334 15. Piggot TJ, Holdbrook DA, Khalid S. Electroporation of the E. coli and S. aureus
335 membranes: Molecular dynamics simulations of complex bacterial membranes. *J*
336 *Physic Chemi B.* **115**(45) (2011).
- 337 16. Kim W, Zhu W, Hendricks GL, et al. A new class of synthetic retinoid antibiotics
338 effective against bacterial persisters. *Nature.* 2018;556(7699).
339 doi:10.1038/nature26157.
- 340 17. Princiotta S, Casciaro B, G. Temprano A, et al. The antimicrobial potential of
341 adarotene derivatives against Staphylococcus aureus strains. *Bioorg Chem.*
342 2024;145. doi:10.1016/j.bioorg.2024.107227.
- 343 18. Witzke S, Petersen M, Carpenter TS, Khalid S. Molecular Dynamics Simulations
344 Reveal the Conformational Flexibility of Lipid II and Its Loose Association with
345 the Defensin Plectasin in the Staphylococcus aureus Membrane. *Biochemistry.*
346 2016;55(23). doi:10.1021/acs.biochem.5b01315.

- 347 19. Joodaki F, Martin LM, Greenfield ML. Generation and Computational
348 Characterization of a Complex *Staphylococcus aureus* Lipid Bilayer. *Langmuir*.
349 2022;38(31). doi:10.1021/acs.langmuir.2c00483.
- 350 20. Abebe AA, Birhanu AG. Methicillin resistant *Staphylococcus aureus*: Molecular
351 mechanisms underlying drug resistance development and novel strategies to
352 combat. *Infect. Drug Resist.* **16**, 7641-7662 (2023).
- 353 21. European Committee on Antimicrobial Susceptibility Testing. European
354 antimicrobial breakpoints. Basel: EUCAST,
355 [https://www.eucast.org/fileadmin/src/media/PDFs/EUCAST_files/Breakpoint table](https://www.eucast.org/fileadmin/src/media/PDFs/EUCAST_files/Breakpoint_table_s/v_14.0_Breakpoint_Tables.pdf)
356 [s/v 14.0 Breakpoint Tables.pdf](https://www.eucast.org/fileadmin/src/media/PDFs/EUCAST_files/Breakpoint_table_s/v_14.0_Breakpoint_Tables.pdf) (2024).
- 357 22. Clinical and Laboratory Standards Institute (CLSI). Performance Standards for
358 Antimicrobial Susceptibility Testing. 34th ed. CLSI supplement M100 (2024).
- 359 23. Ortiz-Miravalles L, Sánchez-Angulo M, Sanz JM, Maestro B. Drug repositioning
360 as a therapeutic strategy against *Streptococcus pneumoniae*: Cell membrane as
361 potential target. *Int. J. Mol. Sci.* 24(6):5831.
- 362 24. Dolan, K. et al. Antifungal activity of tamoxifen: in vitro and in vivo activities and
363 mechanistic characterization. *Antimicrob Agents Chemother.* **53**, 3337-3346 (2009).
- 364 25. Butts, A. et al. Structure-activity relationships for the antifungal activity of selective
365 estrogen receptor antagonists related to tamoxifen. *PLoS One* **10**, e0125927 (2015).
- 366 26. Scott, S. A. et al. Discovery of desketoraloxifene analogues as inhibitors of
367 mammalian, *Pseudomonas aeruginosa*, and nape phospholipase D enzymes. *ACS*
368 *Chem Biol* **10**, 421-432 (2015).
- 369 27. Docobo Pérez, F. Tratamiento de la neumonía experimental por *Staphylococcus*
370 *aureus*. Estudios de eficacia terapéutica de cotrimoxazol, cloxacilina, linezolid y
371 vancomicina frente a cepas *S. aureus* sensible y resistente a meticilin. Ph.D. Thesis,
372 Seville University, Seville, Spain, 26 March 2009.

- 373 28. Christodoulou, M. S. et al. *Synthesis and biological evaluation of novel tamoxifen*
374 *analogues, Bioorg. Med. Chem.* **21**, 4120-4131 (2013).
- 375 29. Christodoulou, M. S. et al. 4-(1,2-diarylbut-1-en-1-yl)isobutyranilide derivatives as
376 inhibitors of topoisomerase II. *Eur. J. Med. Chem.* **118**, 79-89 (2016).
- 377 30. European Committee on Antimicrobial Susceptibility Testing. European
378 antimicrobial breakpoints. Basel: EUCAST,
379 https://www.eucast.org/ast_of_bacteria/mic_determination (2022).
- 380 31. Miró-Canturri, A., Ayerbe-Algaba, R., Villodres, Á. R., Pachón, J. & Smani, Y.
381 Repositioning rafxanide to treat Gram-negative bacilli infections. *J. Antimicrob.*
382 *Chemother.* **75**, 1895-1905 (2020).
- 383 32. Kim S, Lee J, Jo S, Brooks CL, Lee HS, Im W. CHARMM-GUI ligand reader and
384 modeler for CHARMM force field generation of small molecules. *J Comput Chem.*
385 2017;38(21). doi:10.1002/jcc.24829.
- 386 33. Huang J, Rauscher S, Nawrocki G, et al. CHARMM36m: An improved force field
387 for folded and intrinsically disordered proteins. *Nat Methods.* 2016;14(1).
388 doi:10.1038/nmeth.4067.
- 389 34. Lee J, Hitzenberger M, Rieger M, Kern NR, Zacharias M, Im W. CHARMM-GUI
390 supports the Amber force fields. *Journal of Chemical Physics.* 2020;153(3).
391 doi:10.1063/5.0012280.
- 392 35. Lee J, Cheng X, Swails JM, et al. CHARMM-GUI Input Generator for NAMD,
393 GROMACS, AMBER, OpenMM, and CHARMM/OpenMM Simulations Using the
394 CHARMM36 Additive Force Field. *J Chem Theory Comput.* 2016;12(1).
395 doi:10.1021/acs.jctc.5b00935.
- 396 36. Brooks BR, Brooks CL, Mackerell AD, et al. CHARMM: The biomolecular
397 simulation program. *J Comput Chem.* 2009;30(10). doi:10.1002/jcc.21287.

- 398 37. Salomon-Ferrer R, Case DA, Walker RC. An overview of the Amber biomolecular
399 simulation package. *Wiley Interdiscip Rev Comput Mol Sci*. 2013;3(2).
400 doi:10.1002/wcms.1121.
- 401 38. Case DA, Cheatham TE, Darden T, et al. The Amber biomolecular simulation
402 programs. *J Comput Chem*. 2005;26(16). doi:10.1002/jcc.20290.
- 403 39. Roe DR, Cheatham TE. PTRAJ and CPPTRAJ: Software for processing and
404 analysis of molecular dynamics trajectory data. *J Chem Theory Comput*. 2013;9(7).
405 doi:10.1021/ct400341p.
- 406 40. Delano WL. The PyMOL Molecular Graphics System. *CCP4 Newsletter on protein*
407 *crystallography*. 2002;40(1).

408

409 **ACKNOWLEDGMENTS**

410 We thank José María Marimon Ortiz de Zárate for sharing the MRSA clinical isolates,
411 Cayetana Martín and the Proteomic facility of the Andalusian Center of Developmental
412 Biology for their technical help and the COST Action CA21145 – European Network
413 for diagnosis and treatment of antibiotic-resistant bacterial infections (EURESTOP).
414 This work was funded by the Consejería de Universidad, Investigación e Innovación de
415 la Junta de Andalucía (grant ProyExcel_00116).

416

417 **AUTHOR CONTRIBUTIONS**

418 Conceptualization, M.S.C. and Y.S.; methodology, I.M.P., J.F.T., M.S.C., L.C. and
419 S.P.; formal analysis, I.M.P., J.F.T., K.H., M.M. and Y.S.; writing—original draft
420 preparation, I.M.P. and Y.S.; writing-review and editing, M.S.C., M.M., S.D. and Y.S.;
421 funding acquisition, Y.S. All authors have read and agreed to the published version of
422 the manuscript.

423

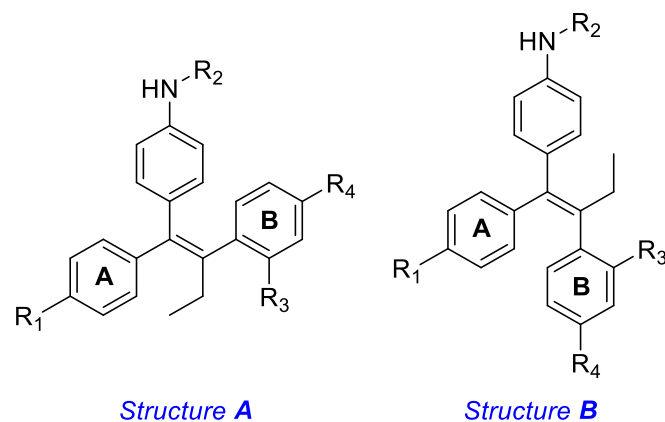
424 **CONFLICTS OF INTEREST**

425 The authors have not conflicts of interest to declare.

426

427

428 **Table 1.** MIC ($\mu\text{g/mL}$) of tamoxifen derivatives **1** – **22** for reference strain of *S. aureus*



429

430

Compound	Structure	R ₁	R ₂	R ₃	R ₄	<i>S. aureus</i> ATCC 1556
1	A	H	H	H	H	>64
2	A	OH	CON(CH ₂ CH ₃) ₂	H	OH	32
3	A	OBn	COCH ₂ CH ₃	H	OBn	>64
4	B	OBn	COCH ₂ CH ₃	H	OBn	>64
5	A	OH	CON(CH ₃) ₂	H	OH	32
6	B	OH	CON(CH ₃) ₂	H	OH	16
7	A	OCH ₃	CO <i>i</i> Propyl	H	H	>64
8	B	OCH ₃	CO <i>i</i> Propyl	H	H	>64
9	A	H	CO <i>i</i> Propyl	H	H	>64

10	B	H	CO <i>i</i> Propyl	H	H	>64
11	B	H	CO <i>i</i> Propyl	H	OBn	>64
12	A	H	CO <i>i</i> Propyl	H	OBn	>64
13	A	OH	CO <i>i</i> Propyl	Cl	Cl	>64
14	B	OH	CO <i>i</i> Propyl	Cl	Cl	>64
15	A	OCH ₃	CO <i>i</i> Propyl	H	OBn	>64
16	B	OCH ₃	CO <i>i</i> Propyl	H	OBn	>64
17	B	OCH ₃	CO <i>i</i> Propyl	H	OH	>64
18	A	OCH ₃	CO <i>i</i> Propyl	H	OH	>64
19	A	OH	CO <i>i</i> Propyl	H	H	>64
20	B	OH	CO <i>i</i> Propyl	H	H	>64
21	A	OBn	CO <i>i</i> Propyl	H	OBn	>64
22	B	OBn	CO <i>i</i> Propyl	H	OBn	>64

431
432
433
434
435

436 **Table 2.** MIC of tamoxifen derivatives **2**, **5** and **6** for clinical isolates for clinical
437 methicillin-resistant *S. aureus*.

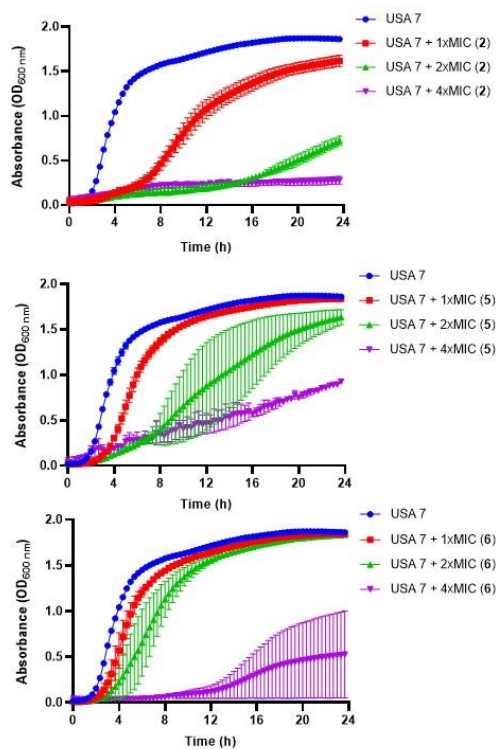
Strain	2	5	6
USA1	32	32	16
USA2	32	64	16
USA3	32	64	16
USA4	32	64	16
USA5	64	64	16
USA6	64	64	16
USA7	32	64	16

438

439

440

441



442

443 **Figure 1. Antibacterial activity of tamoxifen derivatives against clinical**
444 **methicillin-resistant *S. aureus*.** Bacterial growth curves of MRSA USA7 strain in the
445 presence of 1x, 2x and 4xMIC of tamoxifen derivative **2, 5 or 6** for 24 h. Data are
446 represented as mean from two independent. experiments. COL: colistin.

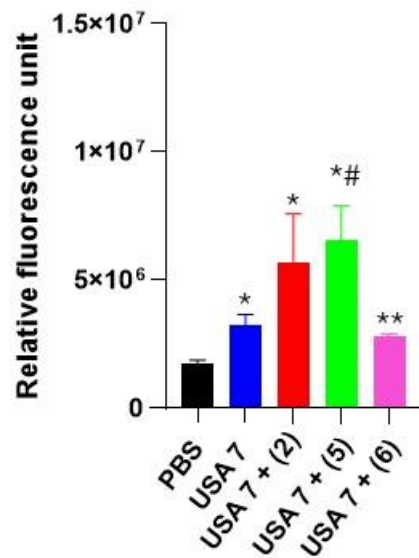
447 .

448

449

450

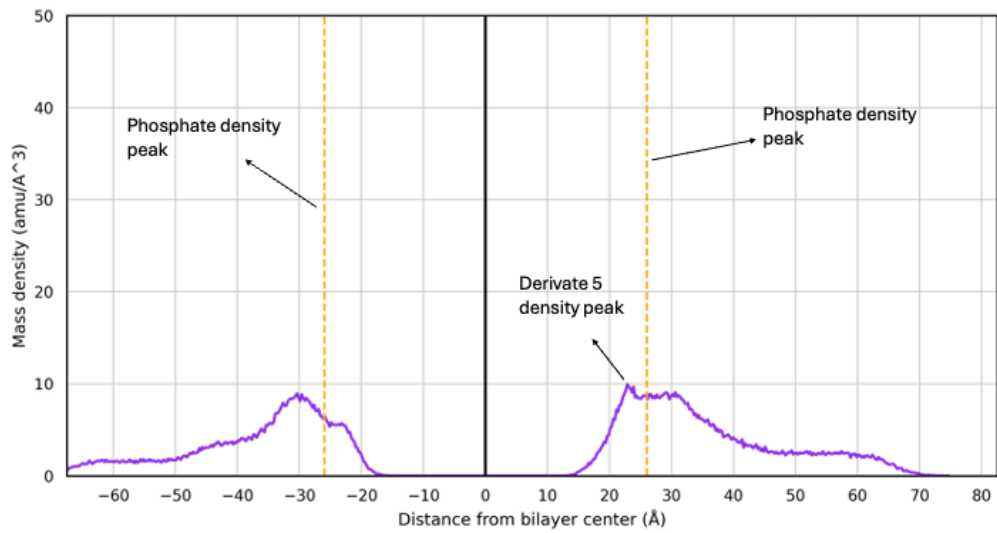
451



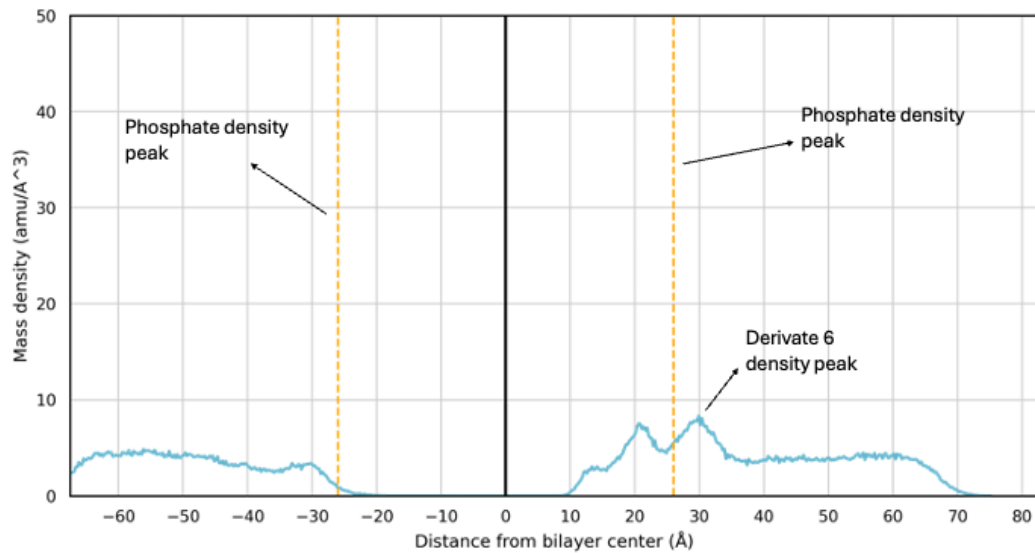
452

453 **Figure 2. Effect of tamoxifen derivatives on the bacterial permeability against**
454 **clinical methicillin-resistant *S. aureus*.** The membrane permeabilization of MRSA
455 USA7 strain in the presence of 1xMIC of tamoxifen derivative **2**, **5** or **6**, incubated for
456 10 min, was quantified by Typhon Scanner. Data are represented as mean \pm SEM from
457 three independent experiments. * $P < 0.05$ vs PBS, # $P < 0.05$ vs USA7, * $P < 0.05$ vs
458 USA7 + (5).

459



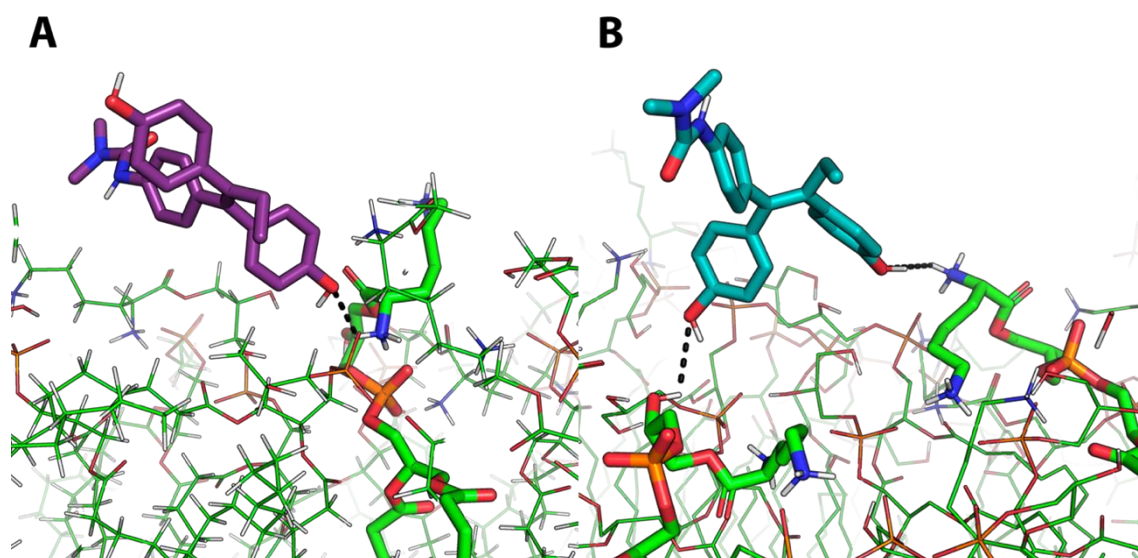
460



461

462 **Figure 3:** Mass density profile of **5 (A)** and **6 (B)** with the corresponding density peaks
463 highlighted. The density peaks of the lipid phosphate groups are shown as orange
464 dashed lines, with maximum density at -26 \AA and $+26 \text{ \AA}$.

465



466

467

468 **Figure 4:** Representative MD frames corresponding to the minimum distances between
469 derivative **5** (**A**, purple sticks) or derivative **6** (**B**, light blue sticks) and the *S. aureus*
470 membrane model. The interactions between these two derivatives and the NH_3^+ moiety
471 (panel **A** and **B**) and $-\text{OH}$ moiety (panel **B**) of phosphatidylglycerol residues is
472 represented by black dashed lines.

473